J Membrane Biol (2013) 246:243–255
DOI 10.1007/s00232-013-9526-y

The Migratory Capacity of Human Trophoblastic BeWo Cells: Effects of Aldosterone and the Epithelial Sodium Channel

G. I. Marino · Y. A. Assef · B. A. Kotsias

Received: 28 July 2012 / Accepted: 8 January 2013 / Published online: 26 January 2013

Abstract Aldosterone is a key regulator of the epithelial sodium channel (ENaC) and stimulates protein methylation on the β-subunit of the ENaC. We found that aldosterone (100 nM) promotes cellular migration in a wound-healing model in trophoblastic BeWo cells. Here, we tested if the positive influence of aldosterone on wound healing is related to methylation reactions. Cell migration and proliferation were measured in BeWo cells at 6 h, when mitosis is still scarce. Cell migration covered 12.4, 25.3, 19.6 and 45.1 % of the wound when cultivated under control, aldosterone (12 h), 8Br-cAMP and aldosterone plus 8Br-cAMP, respectively. Amiloride blocked the effects of aldosterone alone or in the presence of 8Br-cAMP on wound healing. Wound healing decreased in aldosterone (plus 8Br-cAMP) coexposed with the methylation inhibitor 3-deaza-adenosine (3-DZA, 12.9 % reinvasion of the wound). There was an increase in wound healing in aldosterone-, 8Br-cAMP- and 3-DZA-treated cells in the presence of AdoMet, a methyl donor, compared to cells in the absence of AdoMet (27.3 and 12.9 % reinvasion of the wound, respectively). Cell proliferation assessed with the reagent MTT was not changed in any of these treatments, suggesting that cellular migration is the main factor for reinvasion of wound healing. Electrophysiological studies showed an increase in ENaC current in the presence of aldosterone. This effect was higher with 8Br-cAMP, and there was a decrease when 3-DZA was present. AdoMet treatment partially reversed this phenomenon. We suggest that aldosterone positively influences wound healing in BeWo cells, at least in part through methylation of the ENaC.

Keywords BeWo cell · Wound healing · Migration · ENaC · Aldosterone · cAMP · Methylation

G. I. Marino · Y. A. Assef · B. A. Kotsias (✉)
Laboratorio de Canales Iónicos, Instituto de Investigaciones Médicas A. Lanari, IDIM-CONICET, Universidad de Buenos Aires, C. de Malvinas 3150, 1427 Buenos Aires, Argentina
e-mail: kotsias@retina.ar

Introduction

Cell migration is a fundamental process that controls morphogenesis, embryogenesis, immunity, inflammation, tissue regeneration and angiogenesis. Its deregulation causes or is part of many diseases, including autoimmune syndromes, chronic inflammation, mental retardation and cancer. Ion channels and transporters actively participate in this process, being regulated by cytoskeletal components and cell volume (Hoffmann 2011; Riquelme 2011). Epithelial sodium channels (ENaCs) are present in many reabsorbing epithelia and are also expressed in human placenta (del Mónaco et al. 2006, 2008, 2009). Na^+ currents mediated by sodium channels and ENaCs sensitive to amiloride are involved in cell migration and proliferation, which is well documented in epithelial and vascular cells (Chifflet et al. 2005; Grifoni et al. 2006), liver cells (Bondarava et al. 2009) and tumor cells (Sparks et al. 1983; Rooj et al. 2012).

The ENaC is highly regulated. In particular, aldosterone produces an increase in ENaC trafficking and apical membrane expression (Asher et al. 1992; Stokes and Sigmund 1998; Alvarez de la Rosa et al. 2002; Verrey et al. 2008; McEneaney et al. 2008; Butterworth et al. 2005) and an increase in the open probability of the channel (P_o) due to channel activation by proteolysis (Kemendy et al. 1992; Kleyman et al. 2009; Galizia et al. 2011) and to a protein methylation process that has been linked to genomic and

non-genomic activation of the ENaC (Edinger et al. 2006; Zhang et al. 2006; Rokaw et al. 1998). Aldosterone stimulates a carboxymethylation reaction on the ENaC β-subunit, increasing its P_o as a stimulatory effect (Becchetti et al. 2000), which does not require de novo expression of the ENaC subunits (Edinger et al. 2006). Methylation of the β-subunit has been extensively described by other laboratories (Rokaw et al. 1998; Becchetti et al. 2000; Zhang et al. 2006; Edinger et al. 2006). Since the action of aldosterone appears to involve a mechanism that increases the ENaC P_o and this channel participates in BeWo cell migration (del Mónaco et al. 2009), we measured cell migration and proliferation processes associated with wound healing in BeWo cells and chemicals that modify the methylation reactions. The main results are that wound healing is accelerated by aldosterone and cAMP; that 3-deaza-adenosine (3-DZA), an inhibitor of methylation, reduced the healing; and that this was restored by a methyl donor.

Materials and Methods

Cell Culture

The BeWo cell line (American Type Culture Collection, Manassas, VA) was maintained in Ham's F12 medium (GIBCO BRL, Life Technologies, Grand Island, NY) containing 10 % fetal bovine serum (FBS; Natocor Biotechnology, Córdoba, Argentina), 2 mM L-glutamine (Sigma, St. Louis, MO), 100 U/ml penicillin and 100 mg/ml streptomycin. Cells were harvested once a week with 0.25 % trypsin–EDTA (GIBCO BRL, Life Technologies) and kept in an incubator at 37 °C in humid air with constant 5 % CO_2. The endogenous aldosterone concentration in 10 % FBS (0.0152 nM) was insignificant with respect to the aldosterone concentration used in the experiments (100 nM).

Reagents

Aldosterone (Sigma) and progesterone (Sigma) were diluted in ethanol, amiloride (Sigma) was diluted in DMSO and 8Br-cAMP and 3-DZA and AdoMet (Sigma) were diluted in distilled water. Insulin treatment was prepared with NPH human insulin (Humulin N, recombinant DNA technology; Lilly, Neuilly-sur-Seine, France).

Wound-Healing Assay

Cell concentration was adjusted to 2×10^5 cells/cm^2, and cells were seeded onto 24-well plates in Ham's F12 medium containing 10 % FBS, until a confluent cell layer was achieved. Before treatments, the cells to be treated with aldosterone were incubated for 12 h with this hormone (100 nM) and then monolayers were manually scraped with a 200-µl pipette tip and washed with medium without serum to remove non-adherent cells. At this moment, Ham's F12 + 1 % FBS was added to attenuate cellular proliferation without impairing cell survival, with different treatments: (1) a control group with the drug vehicles, (2) 100 nM aldosterone, (3) 100 nM aldosterone plus 100 µM 8Br-cAMP, (4) 100 nM aldosterone and 100 µM 8Br-cAMP plus 10–1,000 µM 3-DZA, (5) 100 nM aldosterone and 100 µM 8Br-cAMP plus 200 µM 3-DZA and 200 µM AdoMet, (6) 100 nM aldosterone plus 10 µM amiloride, (7) 100 nM aldosterone and 100 µM 8Br-cAMP plus 10 µM amiloride, (8) 200 µM 3-DZA and (9) 200 µM AdoMet.

Another group of cells were incubated with (1) the drug vehicles, (2) 20 nM insulin, (3) 1 µM progesterone, (4) 20 nM insulin plus 10 µM amiloride and (5) 1 µM progesterone plus 10 µM amiloride.

All treatments were incubated for 6 h straight without intermediate washes. Cells were cultured at 37 °C with constant 5 % CO_2. Wound scraping was considered time 0 (when treatments were added), and images were taken 6 h after the injury, photographing the same area. Healing was quantified using ImageJ 1.39 software (Image Processing and Analysis in Java; NIH, Bethesda, MD). A mark was made in each well to measure the same spot every time. A straight line was traced in the images, crossing the wound through the denuded area; and the number of pixels was determined using the measuring command of the program. The straight line length expressed in pixels was considered to represent the width of the wound at each time analyzed. Results were expressed as reinvasion percentage of the wound compared to time 0 (mean ± standard deviation).

MTT Assay

Cell proliferation was assessed using the 3-(4,5-dimethylthiazol-2-yl)-2,5-diphenyl tetrazolium bromide (MTT, Sigma) assay. BeWo cells were incubated in 96-well culture plates in Ham's F12 medium with 1 % FBS and grown until confluence. Aldosterone-treated cells were first incubated for 12 h with the hormone, and after this they were tested for 2 h with the same first pool of treatments as described in the wound-healing experiments. Then, 20 µl of MTT (5 mg/ml in PBS) were added to each monolayer well and incubated for an additional 4 h at 37 °C. At the end the MTT formazan precipitate was dissolved in 100 µl of DMSO. Optical density was measured at 570 nm (OD_{570nm}) on an ELISA plate reader (R&D Systems, Minneapolis, MN), and cell proliferation was calculated as a percentage of control (treated cultures OD_{570nm}/control

cultures OD_{570nm} × 100) and expressed as mean ± standard deviation.

Whole-Cell Recordings

Electrophysiological studies were carried out as described previously (del Mónaco et al. 2008). Briefly, cells were grown on glass coverslips with the different treatments: control, aldosterone, aldosterone plus 200 μM 3-DZA and/or plus 200 μM AdoMet. They were washed with bath solution and transferred into the patch recording chamber mounted on an inverted microscope (Olympus, Tokyo, Japan). We added 100 μM 8Br-cAMP or 10 μM amiloride directly in the bath solution as the experiment required. Electrical activity was recorded in the whole-cell patch-clamp configuration (List L/M-EPC7, 1 GΩ feedback resistor; List Medical Electronics, Darmstadt, Germany). Signals were analyzed using pCLAMP v.8 software (Axon Instruments, Union City, CA). The whole-cell configuration was established with polished glass micropipettes (2–4 MΩ resistance when filled with pipette solution). The series resistance (R_s) was compensated for using the analog circuit of the amplifier. The protocol consisted of pulses from 40 to −140 mV in steps of 20 mV from a holding potential of 0 mV, with a 10-s interval between each pulse. The capacitance of the cells (C_m) was measured by applying 100-ms, 10-mV, depolarizing pulses from a holding potential of 0 mV; and current–voltage (*I–V*) plots measured in the steady state were expressed as current densities (current per unit cell capacitance). Currents were fitted to an exponential function, and the time constant (τ) was measured; thus, $C_m = \tau/R_s$. All experiments were done at room temperature (20–24 °C).

The pipette solution (intracellular) contained (in mM) 82 K-gluconate, 40 Na-gluconate, 6 KCl, 4 $MgCl_2$, 10 HEPES, 3 EGTA and 5 sucrose (pH 7.4). The bath solution contained (in mM) 105 NaCl, 4 KCl, 3 $CaCl_2$, 3 $MgCl_2$, 10 HEPES and 40 sucrose (pH 7.4). The osmolality values, measured with a vapor pressure osmometer (5100B; Wescor, Logan, UT), were 287 ± 9 and 305 ± 2 mOsm/l for the intracellular and extracellular solutions, respectively (four measurements).

Isolation of Total Protein

BeWo cell layers were cultured without and with 100 nM aldosterone for 12 h and then for 4 h with different treatments: (1) a control group with the drug vehicles, (2) 100 nM aldosterone, (3) 100 nM aldosterone plus 100 μM 8Br-cAMP and (4) 100 nM aldosterone and 100 μM 8Br-cAMP plus 200 μM 3-DZA. Cells were washed with PBS buffer (GIBCO BRL, Life Technologies) and scraped into ice-cold PBS buffer with 0.01× protease inhibitor cocktail and 0.2 mM phenylmethanesulfonyl fluoride (Sigma), centrifuged and resuspended in lysis buffer (0.3 M NaCl, 25 mM HEPES, 1.5 mM $MgCl_2$, 0.2 mM EGTA, 1 % Triton X-100 [pH 7.4]) with protease inhibitors. The homogenate was spun for 5 min at 10,000 rpm (4 °C), and the supernatant was collected and stored at −20 °C. Total protein in each sample was quantified using the Bradford protein assay (Bradford reagent, Sigma). Total BeWo protein was dissolved in loading buffer (2 % sodium dodecyl sulfate, 50 mM Tris–HCl [pH 6.8], 100 mM dithiothreitol, 0.02 % bromophenol blue, 10 % glycerol) and heated to 100 °C for 10 min.

Immunoblotting

For immunoblot studies, proteins (75 μg) were resolved on 8 % polyacrylamide gel and electrotransferred onto nitrocellulose membranes (Hybond ECL; Amersham, GE Healthcare, Little Chalfont, UK). Membranes were blocked for 1 h with 2 % (w/v) defatted milk in Tris-buffered saline–Tween 0.1 % (T–TBS) at room temperature and incubated overnight with ENaC antibodies in T–TBS buffer supplemented with 0.5 % (w/v) bovine serum albumin (BSA, Sigma). To detect ENaC subunits, we used rabbit polyclonal antibodies directed against amino acid residues 131–225 of human α-ENaC at a dilution of 1:1,000 and residues 411–520 of human γ-ENaC at a dilution of 1:500 overnight and a mouse monoclonal antibody directed against amino acid residues 271–460 of human β-ENaC at a dilution of 1:500 overnight. All antibodies were from Santa Cruz Biotechnology (Santa Cruz, CA) and used in previous works (del Mónaco et al. 2008, 2009). Actin was detected to estimate relative amounts of total protein loaded in each lane (Santa Cruz Biotechnology). Membranes were washed with T–TBS and incubated for 1 h at room temperature with goat anti-rabbit (for α- and γ-ENaC) or horse anti-mouse (for β-ENaC) secondary antibodies conjugated to horseradish peroxidase (1:5,000) (Vector Lab, Burlingame, CA). Filters were washed and immunoreactivity was detected using the ECL Western Blotting Analysis System (Amersham, GE Healthcare). The chemiluminescence reaction was visualized on AGFA Medical X-Ray films (Agfa-Gevaert, Buenos Aires, Argentina). The relative level of each protein was obtained using the ImageJ 1.37v densitometric software.

Cell Surface Biotinylation

Cell-surface expression levels of ENaC subunits were examined using the membrane-impermeant biotinylation reagent (Pierce Chemical, Rockford, IL). BeWo cells were seeded onto T75 cm^2 flasks up to 90–95 % confluence and

cultured without and with 100 nM aldosterone for 12 h and then for 6 h with different treatments: (1) a control group with the drug vehicles, (2) 100 nM aldosterone, (3) 100 nM aldosterone plus 100 μM 8Br-cAMP and (4) 100 nM aldosterone and 100 μM 8Br-cAMP plus 200 μM 3-DZA. After this, the medium was removed and the cells were washed twice with ice–PBS, pH 8.0. Each flask of cells was incubated with 10 ml of sulfo-NHS-SS-biotin (0.5 mg/ml in PBS) and gently agitated on ice for 30 min at 4 °C. The reagent was freshly prepared for incubation. After biotinylation, each flask was incubated with 500 μl of quenching solution (192 mM glycine, 25 mM Tris–Cl [pH 7.4]) for 20 min on ice to ensure complete quenching of the unreacted sulfo-NHS-SS-biotin. Cells were scraped into solution and pelleted at 500 rpm for 5 min. Pellets were solubilized for 30 min in 150 μM of lysis buffer (500 mM NaCl, 50 mM Tris–Cl, 1 % Triton X-100 and 5 mM EDTA) containing protease inhibitors. Unlysed cells were removed by centrifugation at 13,000 rpm at 4 °C. NeutrAvidin-agarose beads (50 μl, Pierce Chemical) were added to the supernatant to isolate cell membrane protein and incubated overnight in an end-over-end mixing rotator. Membrane proteins were dissolved in loading buffer with 50 mM DTT. ENaC subunits were detected in the pool of surface proteins by polyacrylamide gel electrophoresis and immunoblotting as described above. Biotinylated α-, β-, and γ-ENaC signals were quantified by staining with ponceau red to estimate relative amounts of total protein. Densitometry was performed, and after normalization with ponceau red, the values were plotted as relative abundance of the proteins with respect to control. Each experiment was repeated two or three times.

Statistical Analysis

Data were expressed as mean values ± standard deviation (SD) (n = number of cells analyzed). Statistical analysis was performed using one-way and repeated measures ANOVA for multiple data comparison, followed by a post hoc test (Tukey's or Dunnett's test, when appropriate). Differences were considered statistically significant when $p < 0.05$.

Results

Aldosterone and 8Br-cAMP Increase Wound-Healing Activity

A section of the cell layer was removed with the tip of a micropipette. This action left a clear space on the plastic for the cells to fill, and the wound border served as a migratory start line. This cleared space was subsequently visualized under the microscope and photographed to assess the ability of the cells to migrate and fill the wounded area. When BeWo cells were treated with aldosterone we observed a significant increase in wound healing in comparison with the non-treated cells, as expected by our previous results (del Mónaco et al. 2009) ($p < 0.05$, $n = 12$) (Fig. 1).

8Br-cAMP, an analog of cAMP, increases the apical channel number by recruiting ENaCs from subapical storage pools (Hughey et al. 2003; Harris et al. 2007) and increases channel P_o, the two mechanisms by which cAMP leads to enhanced ENaCs (Yang et al. 2006). To see if 8Br-cAMP would interact synergistically with aldosterone on wound healing, we examined BeWo cells treated with aldosterone (100 nM, 12 h) plus 8Br-cAMP (100 μM, 30 min). The migratory behavior of the cells in aldosterone plus the cAMP analogue was higher in comparison with cells treated only with aldosterone. 8Br-cAMP by itself had a similar effect as with aldosterone alone. In all cases 10 μM amiloride blocked the positive effect of the hormone ($p < 0.05$) (Fig. 1a). The mean values obtained from 12 experiments are shown in Fig. 1b.

We employed, in this work, 100 nM aldosterone, which is in the range studied by others working on ENaCs (10 nM–1.5 μM) (McEneaney et al. 2008; Helms et al. 2005). In some experiments we observed that a lower concentration (10 nM) influenced wound healing only 12 h after injury in comparison with the control treatment: 20.5 ± 0.9 and 15.8 ± 0.3 %, respectively, $n = 10$. Thus, in the rest of the experiments the concentration of aldosterone used was 100 nM. To see if cellular proliferation influenced the wound-healing result, we measured cell proliferation with the MTT assay (Fig. 1b, right panel). With BeWo cells kept in 1 % serum concentration, no changes in cell proliferation were seen in the 6-h culture for any treatment ($p > 0.05$, $n = 15$). Endogenous aldosterone concentration in 1 % FBS (0.00152 nM) is insignificant with respect to the aldosterone concentration used in the experiments (100 or 10 nM in some cases).

Insulin- and Progesterone-Induced Wound Healing

To address the possibility that the activity of ENaC by itself also correlates with the functional rate of wound healing, we tested other modulators of ENaC activity, such as insulin and progesterone, that may have the same effect observed with aldosterone and/or cAMP. In BeWo cells the migratory process in the presence of progesterone (1 μM) or insulin (20 nM) was greater than in their absence. In both cases, 10 μM amiloride blocked the positive effect of the hormones ($p < 0.05$, $n = 4$) (Fig. 1c).

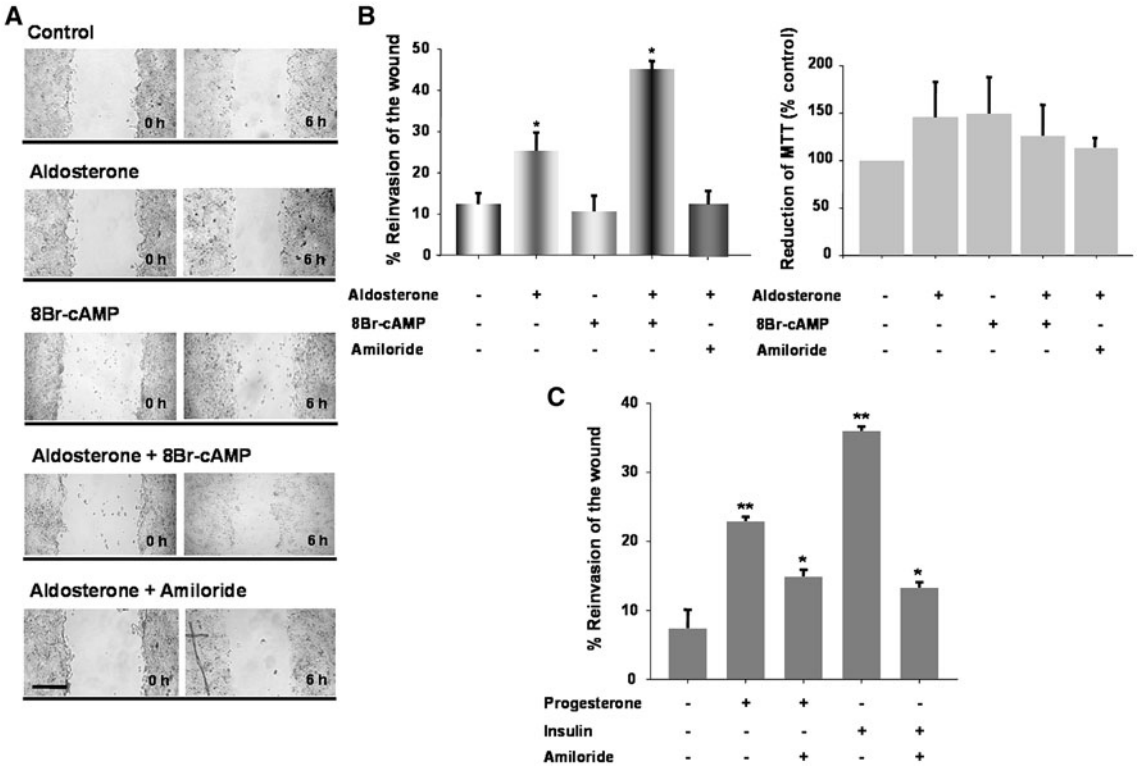

Fig. 1 Wound healing in the presence of aldosterone and 8Br-cAMP. **a** Images of BeWo epithelial sheets cultured under different treatments: control conditions (vehicle), aldosterone 100 nM, 100 μM 8Br-cAMP, 100 nM aldosterone plus 100 μM 8Br-cAMP and aldosterone plus 10 μM amiloride. Pictures were taken when the sheets were wounded by scratching (time 0) and 6 h later. **b** Percentage of reinvasion of the wound for the treatments studied (*left panel*). Aldosterone plus 8Br-cAMP-treated BeWo cells closed a greater percentage of the wound than the rest of the treatments ($p < 0.05$, $n = 12$). The effect of aldosterone was blocked by amiloride. MTT cell viability was assayed for measuring cellular growth. Results are expressed (*right panel*) as a percentage of MTT reduction (compared to control treatment). No difference was observed between the treatments ($p > 0.05$, $n = 15$). **c** Percentage of reinvasion of the wound for insulin- or progesterone-treated BeWo cells in the presence or absence of amiloride ($p < 0.05$, $n = 4$). Significant difference from control: $^{*}p < 0.05$, $^{**}p < 0.01$

Sodium Currents Are Increased by Aldosterone and cAMP

A cAMP signaling pathway regulates the recruitment of ENaCs from subapical storage pools to increase channels in the apical membrane or by increasing the number of channels in the membrane by inhibiting endocytosis (Butterworth et al. 2005) and activates ENaCs, increasing their P_o (Yang et al. 2006). We measured ENaCs with standard whole-cell patch-clamp conditions, testing 100 μM 8Br-cAMP in the presence and absence of aldosterone.

Cells were cultivated in the absence and presence of 100 nM aldosterone for the last 12 h. In some experiments cells were exposed to 100 μM 8Br-cAMP (30 min) and at the end of the experiments to 10 μM amiloride (~10 min, in the presence of 8Br-cAMP). Amiloride-sensitive currents ($I_{Na[amil]}$) were defined as the difference of the current in the absence versus the presence of amiloride. Figure 2a shows current densities for untreated and 100 nM aldosterone-treated cells. It is clear that in cells incubated with aldosterone the current increment was greater than in cells not treated with aldosterone and that this increment was abolished with 10 μM amiloride. Currents in aldosterone and 8Br-cAMP (Fig. 2a, c) were larger than those in control cells, and the combination of 8Br-cAMP together with aldosterone produced a much larger increment in $I_{Na[amil]}$ than with each drug alone. The average results of $I_{Na[amil]}$ relative to control (current per unit cell capacitance, mean $C_m = 31.3 \pm 14.8$ pF, $n = 98$) for a −140-mV pulse are shown in Fig. 2b. The mean reversal potentials (E_{rev}) were 0.5 ± 1.4 and 7.3 ± 3.5 mV for control and 8Br-cAMP plus aldosterone-treated cells, respectively ($p < 0.05$), indicating that cAMP and aldosterone shift the E_{rev} to more positive values. With the solutions used in these experiments the theoretical E_{Na} is 24 mV and the difference from the experimental value is probably due to a limited K^+ permeability through this channel (del Mónaco et al. 2008).

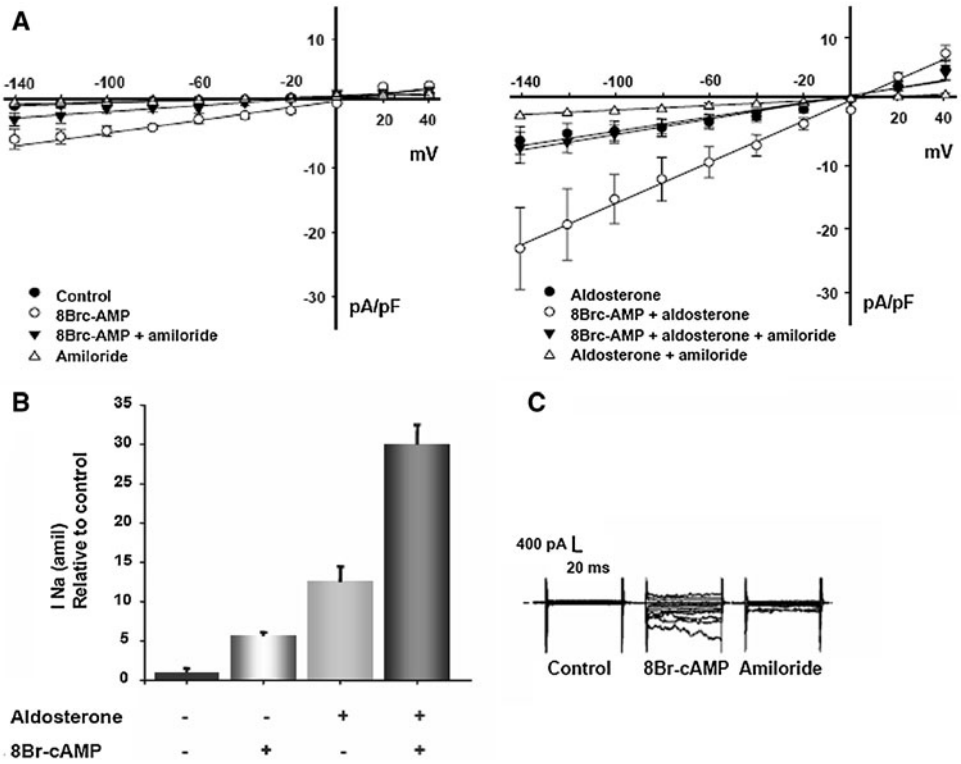

Fig. 2 Whole-cell currents in the presence of aldosterone and cAMP. **a** Average current densities (current per unit cell capacitance vs. voltages) from cells cultured without (*left panel*) and with (*right panel*) 100 nM aldosterone. Current densities were measured before and after stimulation with 100 μM 8Br-cAMP and after addition of 10 μM amiloride. Cells in aldosterone showed larger currents than those in the absence of the hormone, and this difference increased in the presence of 8Br-cAMP. The blocking effect of amiloride is also evident. **b** Four groups of cells were used: one treated with aldosterone-free medium, a second treated with aldosterone-free medium and 100 μM 8Br-cAMP, a third treated with 100 nM aldosterone medium and a fourth treated with 100 nM aldosterone and 100 μM 8Br-cAMP. Current densities were measured before and after adding 10 μM amiloride to the bath solution. Amiloride-sensitive current ($I_{Na[amil]}$) for the pulse of −140 mV was relativized to control (without aldosterone). Both aldosterone and cAMP separately showed a significant increase in currents with respect to control. When the two stimuli were together the current increase was much higher than with the other treatments ($p < 0.05$, $n = 6$). **c** Representative current traces of one experiment of a cell incubated in 100 nM aldosterone before and after 8Br-cAMP and the effects of amiloride

DZA Decreases Percent Reinvasion of the Wound in a Concentration-Dependent Manner

It is known that aldosterone leads to methylation of ENaC, results obtained with the inhibitor of carboxymethylation reactions 3-DZA, which blocks aldosterone effects in other systems (Edinger et al. 2006; Zhang et al. 2006; Rokaw et al. 1998; Becchetti et al. 2000). 3-DZA is a membrane-permeable drug that blocks transmethylation reactions by specifically inhibiting the enzyme *S*-adenosylhomocysteine hydrolase, thereby promoting the accumulation of *S*-adenosylhomocysteine and deaza-D-adenosylhomocysteine. The accumulation of these products inhibits the AdoMet-dependent methyltransferases. Figure 3a shows images of monolayers and the percent reinvasion of the wound for aldosterone plus 8Br-cAMP-treated BeWo cells in 200 μM of 3-DZA for 2–5 h, an incubation time similar to that used by other authors (Rokaw et al. 1998). Clearly, coadministration of 3-DZA (200 μM) reduced the healing behavior observed for aldosterone plus 8Br-cAMP incubation (12.4 ± 2.7, 45.1 ± 2.0 and 12.9 ± 1.5 % reinvasion of the wound when cells were incubated under control, aldosterone plus 8Br-cAMP and aldosterone–8Br-cAMP plus 3-DZA 200 μM treatments, respectively). The 3-DZA stimuli did not show a difference with control samples, indicating that the blocker reversed the effect of aldosterone. 3-DZA treatment alone did not affect wound healing when compared with control samples (10.0 ± 2.9 % reinvasion of the wound) (Fig. 3b).

Figure 4a shows that 3-DZA reduced BeWo cell reinvasion of the wound in a concentration-dependent manner after 6 h of treatment, with an IC_{50} of 47.5 ± 6.0 μM ($n = 12$). Cell proliferation did not change for any of the tested concentrations of 3-DZA ($p > 0.05$, $n = 11$) (Fig. 4b).

In separate experiments monolayers were exposed to the methyl donor AdoMet, a substrate for the methyltransferase responsible for the methylation reaction in the channel

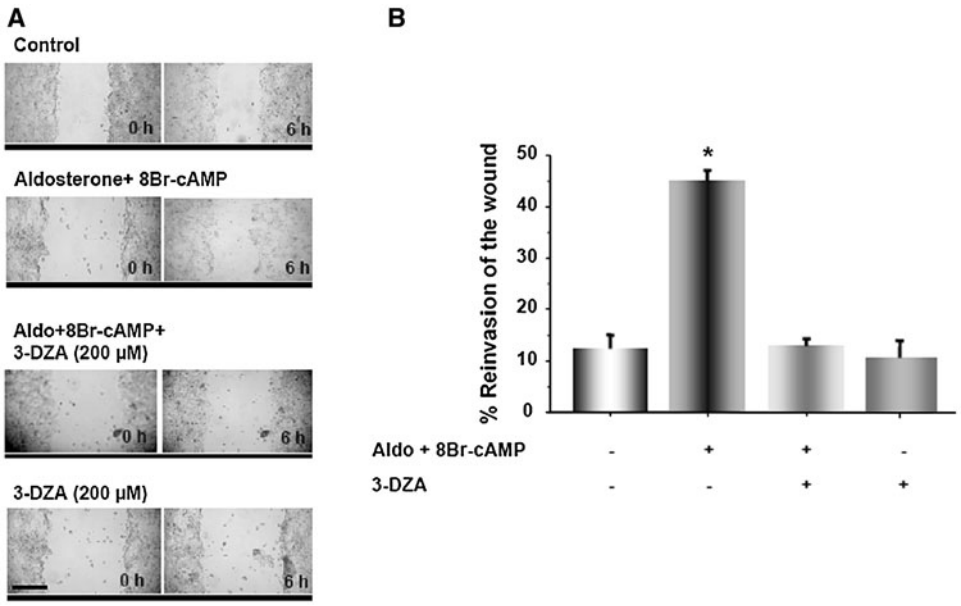

Fig. 3 Wound-healing assay in 3-DZA-treated cells. **a** Images of BeWo epithelial sheets cultured under control conditions (vehicle), aldosterone 100 nM plus 8Br-cAMP 100 μM and aldosterone 100 nM, 8Br-cAMP 100 μM plus 3-DZA 200 μM. **b** Percentage of reinvasion of the wound for treatments studied. 3-DZA-treated BeWo cells closed a lower percentage of the wound than the aldosterone plus 8Br-cAMP treatment ($p < 0.05$, $n = 12$) nearly to control levels. *Asterisk* indicates significant difference with respect to control

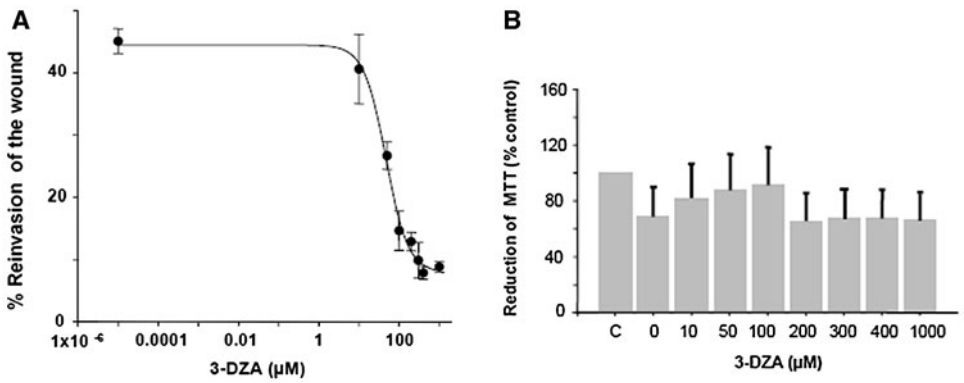

Fig. 4 **a** Effect of various concentrations of 3-DZA (10–1,000 μM) over cellular migration was evaluated by the wound-healing assay in BeWo cells treated with aldosterone 100 nM plus 8Br-cAMP 100 μM. We observed decreased cellular migration with 3-DZA after 6 h of incubation. The 3-DZA concentration on cellular migration reduced by half (IC_{50}) was 47.5 ± 6.0 μM with respect to control (vehicle). The concentration–response curve was representative of 12 separate experiments. **b** Cell proliferation was analyzed after 6 h of incubation with the indicated increasing 3-DZA concentration by MTT assay ($p > 0.05$, $n = 11$)

and in other cellular components that might affect protein expression. Figure 5 shows photographs of monolayers and the percent reinvasion of the wound for aldosterone plus 8Br-cAMP, aldosterone plus 8Br-cAMP plus 3-DZA and BeWo cells coexposed with 200 μM of AdoMet. There was a significant increase in wound-healing behavior in aldosterone-, 8Br-cAMP- and 3-DZA-treated cells in the presence of 200 μM AdoMet (2–5 h) compared to cells in the absence of the methyl donor (27.3 ± 2.4 and 12.9 ± 1.5 % reinvasion of the wound, respectively; $p < 0.05$) (Fig. 5). AdoMet alone did not have any effect on wound healing (10.6 ± 2.0 % reinvasion of the wound, Fig. 5b). As with the former experiments, none of the treatments induced a significant change in cell proliferation.

DZA Reduces Amiloride-Sensitive Currents

To further assess the methylation effect (Rokaw et al. 1998; Becchetti et al. 2000; Zhang et al. 2006; Edinger et al. 2006), ENaC activity was evaluated in aldosterone-treated BeWo cells with 200 μM 3-DZA (2–5 h). Figure 6a

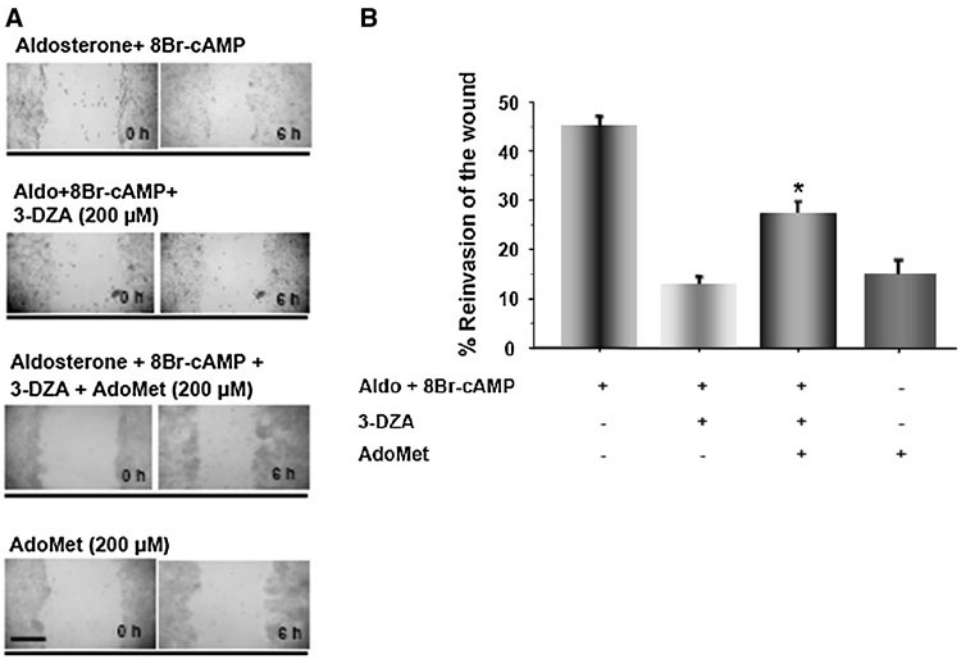

Fig. 5 Wound-healing assay in the presence of AdoMet. **a** Images of BeWo epithelial sheets cultured under 100 nM aldosterone plus 100 µM 8Br-cAMP, in the these same conditions plus 3-DZA 200 µM and in these same conditions plus AdoMet 200 µM. **b** Percentage of reinvasion of the wound for treatments studied. AdoMet closed a higher percentage of the wound than the 3-DZA treatment ($p < 0.05$, $n = 10$). *Asterisk* indicates significant difference with respect to 3-DZA treatment

shows current densities measured after stimulation with 100 µM 8Br-cAMP. In these conditions currents in the presence of 3-DZA were smaller than those in the absence of the blocker (Figs. 2a, 6a, left panel; $p < 0.05$), and they were blocked by 10 µM amiloride. On the other hand, in cells treated with 200 µM AdoMet (plus 3-DZA) there was an increase in the currents compared to cells treated only with 3-DZA (Fig. 6a, right panel). The $I_{Na[amil]}$ had a mean of −15.0, −7.0 and −13.0 pA/pF for the −140-mV pulse in control conditions, 3-DZA and AdoMet, respectively (Fig. 6b). The E_{rev} of the $I_{Na[amil]}$ calculated from the *I–V* curves in aldosterone plus 8Br-cAMP was 8.0 ± 6.7 mV with AdoMet, inducing a significant shift of E_{rev} to more positive values.

We examined whether 3-DZA affected the total expression of ENaC subunits over the time course of aldosterone action. Figure 7a shows bands of the expected size for ENaC subunits, including band doublets for α- and γ-ENaC that apparently result from protein cleavage: ~95 and ~30 kDa for α-ENaC and ~95 and ~75 kDa for γ-ENaC (del Mónaco et al. 2008; Hughey et al. 2003; Harris et al. 2007). None of the treatments induced a significant difference in the ~95- and ~93-kDa fragments corresponding to the full-length of α- and γ-ENaC subunits, nor in the two cleavage products, ~30 and ~75 kDa, respectively (Fig. 7a, left and right panels). The ~100-kDa band for β-ENaC also showed no changes for any treatments applied (Fig. 7a, middle panel).

Biotinylation of the BeWo membrane was used to estimate whether the applied treatments could modify the cell-surface expression of the three ENaC subunits. The biotinylated α-, β- and γ-ENaC protein was detected as a single band of ~30, ~100 and ~75 kDa, respectively. Exposure to aldosterone increased the abundance of the subunits of ENaC in the membrane compared with control conditions. However, there was no difference in cell-surface expression of the subunits between any of the treatments (aldosterone, aldosterone plus cAMP and aldosterone plus cAMP and 3DZA) (Fig. 7b).

Discussion

This work shows that aldosterone and 8Br-cAMP influenced wound healing in BeWo cells through an effect upon the ENaC. In addition, migration and ENaC activity decreased with the methylation inhibitor 3-DZA, this effect being partially reversed with the methyl donor *S*-adenosylmethionine (AdoMet). These results are an extension of previous findings showing that anti-sense oligonucleotides against ENaC abolished the aldosterone effect on cell migration and Na^+ current through ENaC (del Mónaco et al. 2009).

In response to injury, epithelial cells migrate across the wound; and this response requires a range of processes acting from the inside and outside of the cell such as directional

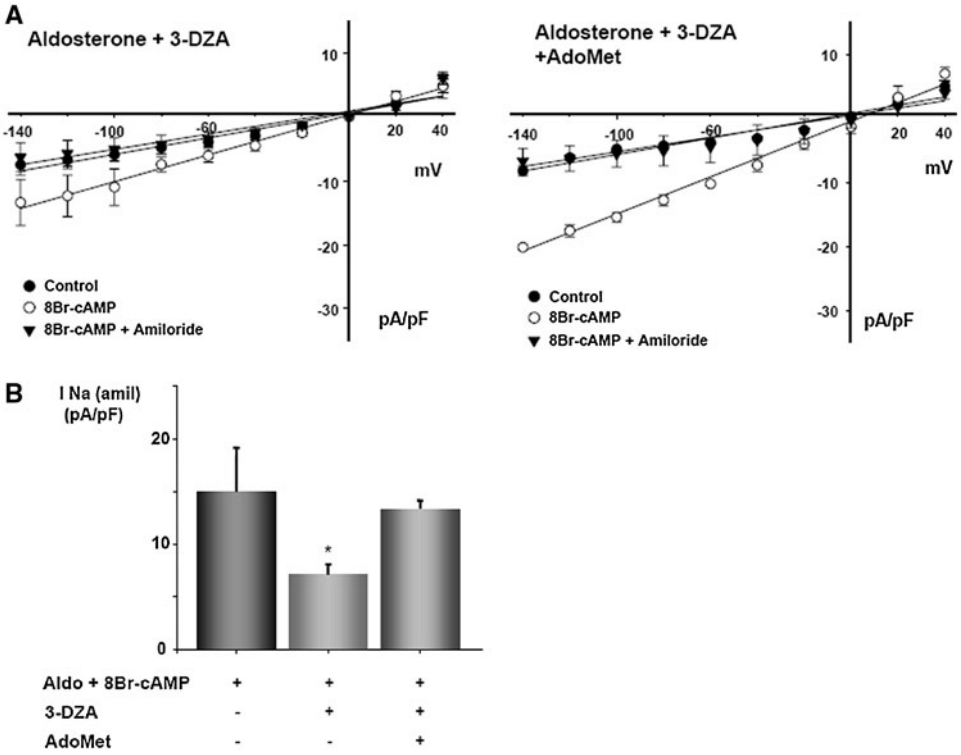

Fig. 6 Whole-cell currents in 3-DZA- and AdoMet-treated BeWo cells. **a** *Left panel I–V* plot for BeWo cells cultured with aldosterone and 200 μM 3-DZA maintained under control conditions, in the presence of 8Br-cAMP and with 8Br-cAMP plus amiloride ($n = 5$). 3-DZA-treated cells showed a reduction in current activation with respect to untreated cells in every pulse applied when exposed to 8Br-cAMP. *Right panel I–V* plot for BeWo cells cultured with aldosterone and 200 μM 3-DZA in the presence of 200 μM AdoMet ($n = 3$). AdoMet treatment showed a partial increase in current activation compared with cells only treated with aldosterone plus 8Br-cAMP. **b** Amiloride-sensitive current ($I_{Na[amil]}$; pA/pF, median ± SD) for the pulse of −140 mV in cells treated with aldosterone and 8Br-cAMP in the presence of 3-DZA and/or AdoMet. *Asterisk* indicates significant difference with respect to aldosterone plus 8Br-cAMP treatment

motility, chemotaxis and mechanotransduction. A growing body of evidence suggests that ENaCs may function as mechanosensors, interacting with the cytoskeleton and the extracellular matrix (Smith et al. 1991; Cantiello et al. 1991; Mazzochi et al. 2006) and generating a mechanically gated Na^+ influx which triggers a secondary signal-transduction pathway (Carattino et al. 2004; Drummond et al. 2004; Wei et al. 2007). According to this, Na^+ entering the cells through ENaCs could be a signal before cells start to migrate. This movement in conjunction with the transport of anions and the consequent water movements may favor the cell swelling required for lamellipodium expansion (Kirk 2010; Kapoor et al. 2009). Chifflet et al. (2005) suggested an alternative explanation with the idea that the depolarization generated by the ENaC stimulates cytoskeletal reorganization, thus promoting wound healing. At least with the cells stimulated with 8Br-cAMP, we cannot rule out the participation of other currents in wound healing because chloride channels like CFTR and ORCC and non-selective cation channels are activated by cAMP pathways and are present in BeWo cells (Marino et al. 2010; Ramos et al. 2008). The migratory behavior in the presence of progesterone or insulin increased two to three times with respect to control, although the effect of amiloride was partial. The reduced effect of the blocker can be explained if there is a factor, independent of the modulation of ENaC by aldosterone and/or cAMP, that contributes to the migratory process. Insulin has been shown in many tissues and model cells to increase Na^+ transport, in part by inducing the translocation of ENaCs to the apical membrane and an increase in the channel activity (Butterworth et al. 2009; Baquero and Gilbertson 2011). Thus, it is known that this hormone stimulates the wound healing and migration of different cell types by signaling pathways (Lima et al. 2012). Progesterone also increases Na^+ transport by enhancing the expression and activity of ENaCs (Laube et al. 2011), but it can downregulate channel P_o (Michlig et al. 2005) and promote wound healing in some systems (Zhao et al. 2010) or inhibit transition from an epithelial to a more invasive phenotype (van der Horst et al. 2012).

BeWo cells treated with aldosterone show amiloride-sensitive currents regulated by aldosterone and a cAMP-sensitive component. They were non-rectifying and reversed at positive potentials, suggesting that Na^+ moves along its electrochemical gradient, shifting the *I–V* plot toward positive potentials. Unstimulated BeWo cells do not show amiloride-sensitive Na^+ currents (Fig. 2), but

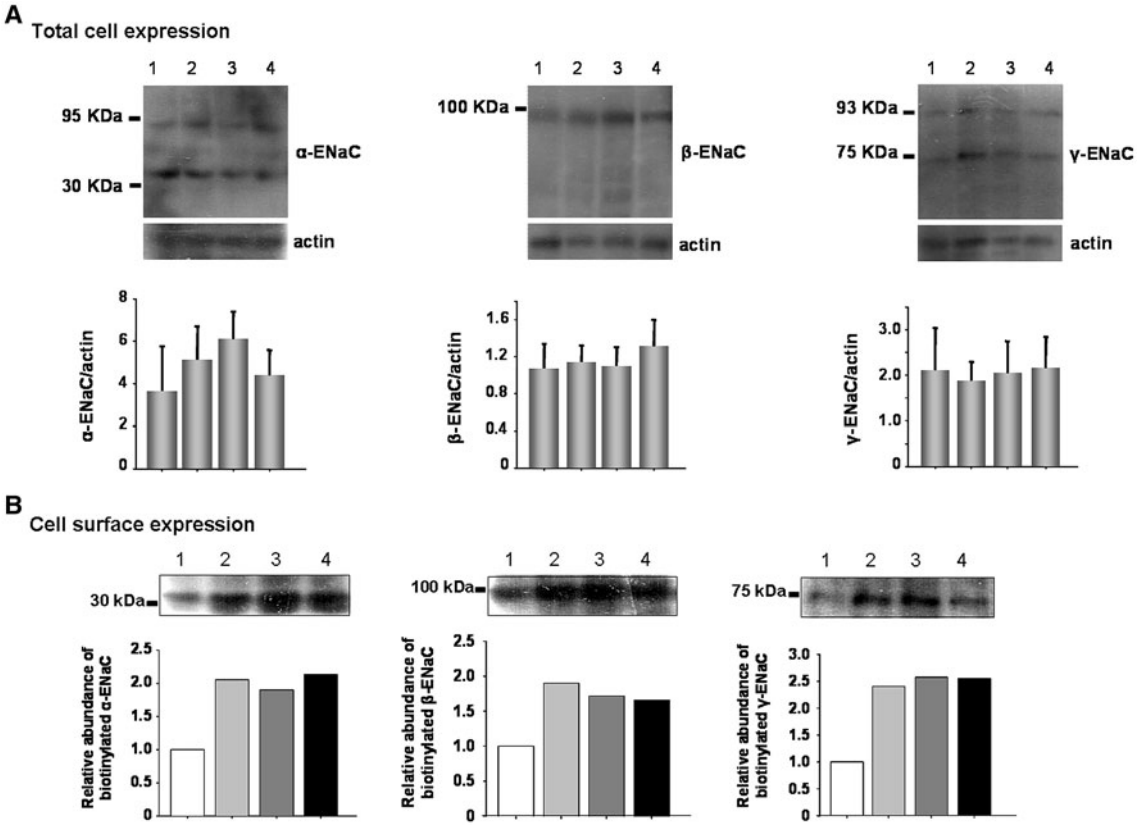

Fig. 7 3-DZA does not inhibit protein expression. **a** α-, β- and γ-ENaC subunits were analyzed by western blotting of total lysates from BeWo cells after each treatment: control conditions (*lanes 1*); supplemented with 100 nM aldosterone for 12 h (*lanes 2*); with aldosterone and 8Br-cAMP 100 μM for 30 min (*lanes 3*); and with aldosterone, 8Br-cAMP and 3-DZA 200 μM for 5 h (*lanes 4*). 3-DZA-treated cells did not show significant changes in the expression of any of the three subunits. The α- and γ-ENaC polypeptides correspond to the whole protein (larger band) and N- and C-terminal proteolytic fragments, respectively, observed previously by our group (del Mónaco et al. 2009). The relative level of the protein in each treatment using actin as an internal control is represented in the *bottom bar graph* ($n = 4$). **b** Western blot analysis of cell-surface expression of α-, β- and γ-ENaC subunits in cells treated as shown in **a**. *Bottom* The intensity of the ENaC subunit expression from the experiments shown at *top* was quantified using ponceau red staining in each lane. Values were plotted as relative abundance of ENaC with respect to control. Each *plotted value* corresponds to one representative experiment from each subunit, but it was repeated at least twice. Aldosterone-treated cells showed significant changes in the expression of the three subunits with respect to control; no differences were recorded between treatments

the total amount of the three ENaC subunits is not different from the hormone-stimulated cells. However, we found that in the presence of aldosterone expression in the cell membrane of the three subunits was increased (Fig. 7), so the observed effect of aldosterone could be due even to an increase in the probability that the channel is open as most plasma membrane expression. In a number of studies of the long-term action of aldosterone, a significant increase in the expression and redistribution from the intracellular localization to the membrane of any ENaC subunit was detected only after 15 h (Butterworth et al. 2009). The higher increment in wound healing observed when both aldosterone and 8Br-cAMP are present may be due to an increase in channel P_o combined with an increase in channel surface expression, the two mechanisms by which cAMP leads to enhanced ENaCs (Butterworth et al. 2005; Yang et al. 2006). Our biotinylation results suggest that cAMP activates ENaC by an increase in the P_o of BeWo cells. However, we cannot exclude that a small increase in membrane protein in cAMP-treated cells, which we were unable to show in the biotinylation experiment, can result in a large increase in the level of activity of ENaCs. The P_o and the number of channels inserted in the membrane are the key components of hormone regulation with incubation time used in our experiments. Acute activation of ENaCs by aldosterone not depending on the mineralocorticoid receptor was reported in *Xenopus* A6 kidney cells (Becchetti et al. 2000) and in rabbit, but not in rat, principal cells (Zhou and Bubien 2001). In addition, biochemical methods support the observation that ENaC mRNA and protein do not increase in the presence of aldosterone in the first 2–4 h when the increase in Na^+ transport and P_o is most dramatic (Becchetti et al. 2000; Asher et al. 1996).

The idea that methylation reactions are required for normal ENaC activity has been proposed by Edinger et al. (2006), who found in kidney cells a novel methyltransferase which contains an AdoMet binding motif that stimulates ENaC activity. We are aware that the methylation effect could involve more than one possible substrate, although at this time we do not have at hand tools to test this hypothesis other than 3-DZA and AdoMet. When 3-DZA-treated cells, in the presence of aldosterone plus 8Br-cAMP, were cultured in 1 % FBS, the reinvasion of the wound measured 6 h after the injury was about 10 % of its initial value, while there was a reinvasion of 45 % in cells cultured only with aldosterone and 8Br-cAMP and 3-DZA by itself did not have any effect on wound healing. 3-DZA blocked the stimulation of Na^+ transport induced by aldosterone and cAMP without affecting cellular amounts (total membrane) of any ENaC subunits, suggesting that the stimulation by methylation occurred as a posttranslational process that resulted in changes in ENaC kinetics.

Initial reports regarding the mechanism of 3-DZA methylation inhibition indicate a rapid reduction (minutes) of sodium transport measured in vesicles of A6 cells (Sariban-Sohraby et al. 1984), although later electrophysiological approaches demonstrated a delay in the inhibition of ENaC currents after hours of incubation (Edinger et al. 2006; Zhang et al. 2006; Rokaw et al. 1998; Becchetti et al. 2000). Even though Becchetti et al. (2000) found that a high concentration of aldosterone (1.5 μM) acutely stimulates ENaC currents, we cultured the cells with 3-DZA and AdoMet for 2–5 h, the temporal window in which the effect of aldosterone on BeWo wound-healing behavior was evident in this report. We show that the effect of 3-DZA reverts when AdoMet is present, although it does not restore the currents to basal levels. Cell membranes have usually a low permeability to AdoMet and to have a higher concentration requires a permeabilized cell (Sariban-Sohraby et al. 1984; Sariban-Sohraby personal communication), which was not the case with the BeWo cells we used.

Although in our experiments the extent of wound healing clearly correlated with ENaC activity under the different treatment conditions, it would be interesting in the future to study the status of methylation per se, which could not be performed at this time because we did not have the facilities to measure the methylation process in a more direct form such as mass spectrometry or cell labeling with [methyl-^{3}H]-L-methionine. However, methylation of the β-subunit of ENaC has been extensively described by other laboratories, as mentioned above.

Cellular proliferation could mask the contribution of migration to wound healing. To test this, we measured cell proliferation with the MTT assay. In a homogeneous sample of cells (like the BeWo cell line), MTT reduction is proportional to the number of metabolically active cells and is used as an indicator of proliferation or viability. Our results show that none of the treatments induced the proliferation of BeWo cells cultured in 1 % FBS concentration for 6 h, although it has been observed that aldosterone stimulates the proliferation of cardiac fibroblasts (Stockhand and Meszaros 2002).

It is known that aldosterone concentration in plasma increases during pregnancy and is reduced by about 50 % in preeclamptic women (Langer et al. 1998; Shojaati et al. 2004). The causes of this syndrome are not known (Huppertz 2008; Knöfler and Pollheimer 2012), but one of the mechanisms proposed is a diminished trophoblast invasion so that the cells invade the maternal tissues at a lesser rate (Redline and Patterson 1995; Nadeem et al. 2011). In this regard it is important to note that treatment of BeWo cells with the methyltransferase inhibitor azathioprine (AZA) resulted in conversion of cell morphology to a non-migratory type (Rahnama et al. 2009). Although our studies were performed in vitro in a trophoblastic cell line, the results presented here may be related to this pathological condition.

Acknowledgments We thank S. del Mónaco and L. Galizia for help and useful discussion of the data. This work was supported by grants from the University of Buenos Aires, National Research Council (CONICET) and Ministerio de Ciencia, Tecnología e Innovación Productiva.

References

Alvarez de la Rosa D, Li H, Canessa CM (2002) Effects of aldosterone on biosynthesis, traffic, and functional expression of epithelial sodium channels in A6 cells. J Gen Physiol 119:427–442

Asher C, Eren R, Kahn L, Yeger O, Garty H (1992) Expression of the amiloride-blockable Na^+ by RNA from control versus aldosterone-stimulated tissue. J Biol Chem 267:16061–16065

Asher C, Wald H, Rossier BC, Garty H (1996) Aldosterone-induced increase in the abundance of Na^+ channel subunits. Am J Physiol Cell Physiol 271:C605–C611

Baquero AF, Gilbertson TA (2011) Insulin activates epithelial sodium channel (ENaC) via phosphoinositide 3-kinase in mammalian taste receptor cells. Am J Physiol Cell Physiol 300:C860–C871

Becchetti A, Kemendy AE, Stockand JD, Sariban-Sohraby S, Eaton DC (2000) Methylation increases the open probability of the epithelial sodium channel in A6 epithelia. J Biol Chem 275:16550–16559

Bondarava M, Li T, Endl E, Wehner F (2009) Alpha-ENaC is a functional element of the hypertonicity-induced cation channel in HepG2 cells and it mediates proliferation. Pflug Arch 458:675–687

Butterworth MB, Edinger RS, Johnson JP, Frizzell RA (2005) Acute ENaC stimulation by cAMP in a kidney cell line is mediated by exocytic insertion from a recycling channel pool. J Gen Physiol 125:81–101

Butterworth MB, Edinger RS, Frizzell RA, Johnson JP (2009) Regulation of the epithelial sodium channel by membrane trafficking. Am J Physiol Ren Physiol 296:F10–F24

Cantiello HF, Stow JL, Prat AG, Ausiello DA (1991) Actin filaments regulate epithelial Na^+ channel activity. Am J Physiol Cell Physiol 261:C882–C888

Carattino MD, Sheng S, Kleyman TR (2004) Epithelial Na^+ channels are activated by laminar shear stress. J Biol Chem 279:4120–4126

Chifflet S, Hernández JA, Grasso S (2005) A possible role for membrane depolarization in epithelial wound healing. Am J Physiol Cell Physiol 288:C1420–C1430

del Mónaco S, Assef Y, Damiano A, Zotta E, Ibarra C, Kotsias BA (2006) Caracterización del canal epitelial de Na en sinciciotrofoblasto de placenta humana preeclámptica. Medicina 66:31–35

del Mónaco SM, Assef YA, Kotsias BA (2008) Epithelial sodium channel in a human trophoblast cell line (BeWo). J Membr Biol 223:127–139

del Mónaco SM, Marino GI, Assef YA, Damiano AE, Kotsias BA (2009) Cell migration in BeWo cells and the role of ENaC channels. J Membr Biol 232:1–13

Drummond HA, Gebremedhin D, Harder DR (2004) Mechanosensor degenerin/epithelial Na^+ channel proteins: components of a vascular mechanosensor. Hypertension 44:643–648

Edinger RS, Yospin J, Perry C et al (2006) Regulation of epithelial Na channels (ENaC) by methylation, a novel methyltransferase stimulates ENaC activity. J Biol Chem 281:9110–9117

Galizia L, Ojea A, Kotsias BA (2011) Amiloride sensitive sodium channels (ENaC) and their regulation by proteases. Medicina 71:179–182

Grifoni SC, Gannon KP, Stec DE, Drummond HA (2006) ENaC proteins contribute to VSMC migration. Am J Physiol Heart Circ Physiol 291:H3076–H3086

Harris M, Firsov D, Vuagniaux G, Stutts MJ, Rossier BC (2007) A novel neutrophil elastase inhibitor prevents elastase activation and surface cleavage of the epithelial sodium channel expressed in *Xenopus laevis* oocytes. J Biol Chem 282:58–64

Helms MN, Yu L, Malik B, Kleinhenz DJ, Hart CM, Eaton DC (2005) Role of SGK1 in nitric oxide inhibition of ENaC in Na^+-transporting epithelia. Am J Physiol Cell Physiol 289:C717–C726

Hoffmann EK (2011) Ion channels involved in cell volume regulation: effects on migration, proliferation, and programmed cell death in non adherent EAT cells and adherent ELA cells. Cell Physiol Biochem 28:1061–1078

Hughey RP, Mueller GM, Bruns JB et al (2003) Maturation of the epithelial Na^+ channel involves proteolytic processing of the alpha- and gamma-subunits. J Biol Chem 278:37073–37082

Huppertz B (2008) Placental origins of preeclampsia: challenging the current hypothesis. Hypertension 51:970–975

Kapoor N, Bartoszewski R, Qadri YJ et al (2009) Knockdown of ASIC1 and ENaC subunits inhibits glioblastoma whole cell current and cell migration. J Biol Chem 284:24526–24541

Kemendy AE, Kleyman TR, Eaton DC (1992) Aldosterone alters the open probability of amiloride-blockable sodium channels in A6 epithelia. Am J Physiol Cell Physiol 263:C825–C837

Kirk KL (2010) CFTR channels and wound healing. Focus on "Cystic fibrosis transmembrane conductance regulator is involved in airway epithelial wound repair". Am J Physiol Cell Physiol 299:C888–C890

Kleyman TR, Carattino MD, Hughey RP (2009) ENaC at the cutting edge: regulation of epithelial sodium channels by proteases. J Biol Chem 284:20447–20451

Knöfler M, Pollheimer J (2012) IFPA Award in Placentology Lecture: molecular regulation of human trophoblast invasion. Placenta 33(Suppl):S55–S62

Langer B, Grima M, Coquard C, Bader AM, Schlaeder G, Imbs JL (1998) Plasma active renin, angiotensin I, and angiotensin II during pregnancy and in preeclampsia. Obstet Gynecol 91:196–202

Laube M, Küppers E, Thome UH (2011) Modulation of sodium transport in alveolar epithelial cells by estradiol and progesterone. Pediatr Res 69:200–205

Lima MH, Caricilli AM, de Abreu LL et al (2012) Topical insulin accelerates wound healing in diabetes by enhancing the AKT and ERK pathways: a double-blind placebo-controlled clinical trial. PLoS ONE 7:e36974

Marino GI, Assef YA, Kotsias BA (2010) An outwardly rectifying chloride channel in BeWo choriocarcinoma cell line. Placenta 31:1093–1100

Mazzochi C, Bubien JK, Smith PR, Benos DJ (2006) The carboxyl terminus of the alpha-subunit of the amiloride-sensitive epithelial sodium channel binds to F-actin. J Biol Chem 281:6528–6538

McEneaney V, Harvey BJ, Thomas W (2008) Aldosterone regulates rapid trafficking of epithelial sodium channel subunits in renal cortical collecting duct cells via protein kinase D activation. Mol Endocrinol 22:881–892

Michlig S, Harris M, Loffing J, Rossier BC, Firsov D (2005) Progesterone down-regulates the open probability of the amiloride-sensitive epithelial sodium channel via a Nedd4-2-dependent mechanism. J Biol Chem 280:38264–38270

Nadeem L, Munir S, Fu G et al (2011) Nodal signals through activin receptor-like kinase 7 to inhibit trophoblast migration and invasion: implication in the pathogenesis of preeclampsia. Am J Pathol 178:1177–1189

Rahnama F, Thompson B, Steiner M, Shafiei F, Lobie PE, Mitchell MD (2009) Epigenetic regulation of E-cadherin controls endometrial receptivity. Endocrinology 150:1466–1472

Ramos AJ, Cantero MR, Zhang P et al (2008) Morphological and electrical properties of human trophoblast choriocarcinoma, BeWo cells. Placenta 29:492–502

Redline RW, Patterson P (1995) Pre-eclampsia is associated with an excess of proliferative immature intermediate trophoblast. Hum Pathol 26:594–600

Riquelme G (2011) Placental syncytiotrophoblast membranes domains, subdomains and microdomains. Placenta 32(Suppl 2):S196–S202

Rokaw MD, Wang JM, Edinger RS et al (1998) Carboxyl methylation of the beta subunit of xENaC regulates channel activity. J Biol Chem 273:28746–28751

Rooj AK, McNicholas CM, Bartoszewski R, Bebok Z, Benos DJ, Fuller CM (2012) Glioma-specific cation conductance regulates migration and cell cycle progression. J Biol Chem 287:4053–4065

Sariban-Sohraby S, Burg M, Wiesmann WP, Chiang PK, Johnson JP (1984) Methylation increases sodium transport into A6 apical membrane vesicles: possible mode of aldosterone action. Science 225:745–746

Shojaati K, Causevic M, Kadereit B et al (2004) Evidence for compromised aldosterone synthase enzyme activity in preeclampsia. Kidney Int 66:2322–2328

Smith PR, Saccomani G, Joe EH, Angelides KJ, Benos DJ (1991) Amiloride-sensitive sodium channel is linked to the cytoskeleton in renal epithelial cells. Proc Natl Acad Sci USA 88:6971–6975

Sparks RL, Pool TB, Smith NK, Cameron IL (1983) Effects of amiloride on tumor growth and intracellular element content of tumor cells in vivo. Cancer Res 43:73–77

Stockhand JD, Meszaros JG (2002) Aldosterone stimulates proliferation of cardiac fibroblasts by activating Ki-RasA and MAPK1/2 signaling. Am J Physiol Heart Circ Physiol 284:H176–H184

Stokes JB, Sigmund RD (1998) Regulation of rENaC mRNA by dietary NaCl and steroids: organ, tissue, and steroid heterogeneity. Am J Physiol Cell Physiol 274:C1699–C1707

van der Horst PH, Wang Y, Vandenput I et al (2012) Progesterone inhibits epithelial-to-mesenchymal transition in endometrial cancer. PLoS ONE 7:e30840

Verrey F, Fakitsas P, Adam G, Staub O (2008) Early transcriptional control of ENaC (de)ubiquitylation by aldosterone. Kidney Int 73:691–696

Wei SP, Li XQ, Chou CF et al (2007) Membrane tension modulates the effects of apical cholesterol on the renal epithelial sodium channel. J Membr Biol 220:21–31

Yang LM, Rinke R, Korbmacher C (2006) Stimulation of the epithelial sodium channel (ENaC) by cAMP involves putative ERK phosphorylation sites in the C termini of the channel's beta- and gamma-subunit. J Biol Chem 281:9859–9868

Zhang W, Xia X, Reisenauer MR, Hemenway CS, Kone BC (2006) Dot1a-AF9 complex mediates histone H3 Lys-79 hypermethylation and repression of ENaC alpha in an aldosterone-sensitive manner. J Biol Chem 281:18059–18068

Zhao JJ, Wang X, Huo ZJ, Luo SQ, Xiong JB (2010) Progesterone promotes the proliferation and migration of cultured breast cancer cells. Nan Fang Yi Ke Da Xue Xue Bao 30:443–446

Zhou ZH, Bubien JK (2001) Nongenomic regulation of ENaC by aldosterone. Am J Physiol Cell Physiol 281:C1118–C1130